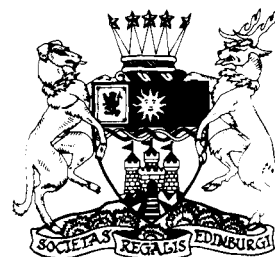


Petrogenesis of slab-derived trondhjemite–tonalite–dacite/adakite magmas

M. S. Drummond, M. J. Defant and P. K. Kepezhinskas

ABSTRACT: The prospect of partial melting of the subducted oceanic crust to produce arc magmatism has been debated for over 30 years. Debate has centred on the physical conditions of slab melting and the lack of a definitive, unambiguous geochemical signature and petrogenetic process. Experimental partial melting data for basalt over a wide range of pressures (1–32 kbar) and temperatures (700–1150°C) have shown that melt compositions are primarily trondhjemite–tonalite–dacite (TTD). High-Al (>15% Al₂O₃ at the 70% SiO₂ level) TTD melts are produced by high-pressure (≥15 kbar) partial melting of basalt, leaving a restite assemblage of garnet + clinopyroxene ± hornblende. A specific Cenozoic high-Al TTD (adakite) contains lower Y, Yb and Sc and higher Sr, Sr/Y, La/Yb and Zr/Sm relative to other TTD types and is interpreted to represent a slab melt under garnet amphibolite to eclogite conditions. High-Al TTD with an adakite-like geochemical character is prevalent in the Archean as the result of a higher geotherm that facilitated slab melting. Cenozoic adakite localities are commonly associated with the subduction of young (<25 Ma), hot oceanic crust, which may provide a slab geotherm (≈9–10°C km⁻¹) conducive for slab dehydration melting. Viable alternative or supporting tectonic effects that may enhance slab melting include highly oblique convergence and resultant high shear stresses and incipient subduction into a pristine hot mantle wedge. The minimum *P–T* conditions for slab melting are interpreted to be 22–26 kbar (75–85 km depth) and 750–800°C. This *P–T* regime is framed by the hornblende dehydration, 10°C/km, and wet basalt melting curves and coincides with numerous potential slab dehydration reactions, such as tremolite, biotite + quartz, serpentine, talc, Mg-chloritoid, paragonite, clinohumite and talc + phengite. Involvement of overthickened (> 50 km) lower continental crust either via direct partial melting or as a contaminant in typical mantle wedge-derived arc magmas has been presented as an alternative to slab melting. However, the intermediate to felsic volcanic and plutonic rocks that involve the lower crust are more highly potassic, enriched in large ion lithophile elements and elevated in Sr isotopic values relative to Cenozoic adakites. Slab-derived adakites, on the other hand, ascend into and react with the mantle wedge and become progressively enriched in MgO, Cr and Ni while retaining their slab melt geochemical signature. Our studies in northern Kamchatka, Russia provide an excellent case example for adakite–mantle interaction and a rare glimpse of trapped slab melt veinlets in Na-metasomatised mantle xenoliths.



KEY WORDS: adakite, trondhjemite, tonalite, dacite, slab melting, Archean, tectonics, mantle metasomatism, Kamchatka.

The focus of granitic rock petrology has leaned towards the study of high-K granites and rhyolites and their relevance to the generation and growth of continental crust through time. This pursuit has allowed us to find that a significant proportion of the granites represent recycling of continental crustal components and contribute sparingly to new net addition for continental crustal growth. To understand the birth of continental crust and its subsequent growth, we should refocus our studies towards the sodic end of the 'granite' family, the trondhjemite–tonalite–dacite group (TTD). Many continental growth models indicate that over 70% of the present day continental crust was produced by the end of the Archean (Armstrong 1981; Dewey & Windley 1981; McLennan & Taylor 1982; Reymer & Schubert 1984), with tonalite–trondhjemite suites constituting 60–70% (Condie 1981) of the preserved Archean crust. Wedepohl (1995) has suggested a tonalitic composition for the bulk continental crust. This may have resulted from ridge subduction, concomitant slab melting and associated TTD generation in the Archean (Martin 1986, 1993; Nelson & Forsythe 1989; Drummond & Defant 1990).

Numerous petrogenetic models, experimental studies and

thermomechanical calculations have sought to explain the role of the subducted oceanic lithosphere in arc magma genesis. Early studies (Green & Ringwood 1968; Marsh & Carmichael 1974) postulated a role for slab melting in the genesis of arc magmatism. More recently it has been argued that, in general, the slab does not melt, but dehydrates, contributing fluids to and enhancing melting conditions in the overlying mantle wedge (e.g. Gill 1981; Mysen 1982; Arculus & Powell 1986; Tatsumi *et al.* 1986; Ellam & Hawkesworth 1988; Kushiro 1990). However, slab and mantle wedge sources need not be mutually exclusive or individually the sole source for arc magmatism.

This paper will evaluate the derivation of sodic, intermediate to felsic igneous rocks from a subducted slab (MORB) source. Although the process of slab melting has persisted through time (Defant & Drummond 1990; Drummond & Defant 1990), the rate of slab melting has slowed dramatically since the Archean. It is the goal of this study to further refine the geochemical characteristics of slab melts and to delimit the physical conditions of slab melting. The geochemical discrimination of slab melts (adakites) from mafic lower crustal melts

is presented to more fully distinguish adakites as a recognisable lithology with important tectonic implications. A mantle geochemical component is recorded in numerous adakite localities due to reaction between adakite melt and sub-arc mantle on ascent. Mantle xenoliths from northern Kamchatka will be used for the analysis of slab melt–mantle interaction. Metasomatism of the mantle wedge by adakite melts presents fundamental information on source heterogeneity for mantle-derived arc magmas.

1. Methods of TTD generation

Models for TTD genesis have been summarised in previous studies (Arth 1979; Barker 1979; Drummond & Defant 1990) and commonly involve either the partial melting of a basaltic source or fractional crystallisation of basaltic parental magma. Partial melting processes are considered to be a more efficient mechanism for TTD production as 80–90% fractional crystallisation is required to produce residual TTD liquids from basaltic (Spulber & Rutherford 1983) or boninitic (Meijer 1983) mantle-derived parental magmas. Many TTD localities lack high proportions of mafic to intermediate igneous rocks, which argues against the fractional crystallisation process as the dominant TTD petrogenetic model.

Experimental studies have shown that partial melting of a basaltic source over a wide range of temperature (700–1150°C) and pressure (1–32 kbar) results in a TTD melt product. Figure 1 shows the distribution of the available basalt partial melt experimental data (170 samples) with respect to the granitic rock subdivision of Barker (1979). Those experimental glasses containing <56% SiO₂ (30 samples, not shown) or >50% normative An proportion (28 samples, Fig. 1) are unlike natural TTD compositions and will not be considered further. Most experimental melt compositions are tonalite (60%), trondhjemite (23%) and granodiorite (12%), with a minor (5%) granite melt representative. Thus the dominant product from partial melting of a low-K₂O basaltic source is represented by the Ab-rich end of the granitic rock spectrum. A first-order screen of the samples under consideration for low-K₂O basalt partial melt genesis should be that the Ab–An–Or data reside primarily in the tonalite–trondhjemite fields.

Drummond and Defant (1990) and Defant and Drummond (1990) defined a specific subtype of Cenozoic TTD (adakite) similar geochemically to Archean high-Al (>15% Al₂O₃ at 70% SiO₂ level) TTD gneisses. Table 1 summarises over 2000 published analyses of continental and island arc andesite–dacite–rhyolite (ADR) suites, low-Al TTD (<15% Al₂O₃ at 70% SiO₂ level), ophiolitic plagiogranites, boninites and the adakite/high-Al TTD group. The low-Al TTD group represents non-ophiolitic, low pressure partial melts of a basaltic source without accompanying mafic to intermediate fractionation products (Barker *et al.* 1976; Drummond & Defant 1990). Qualitative comparison of the Table 1 data indicates that the adakite/high-Al TTD group has elevated Sr, La/Sm, Sr/Y and Zr/Y and depleted Y, Sc and Yb values. This geochemical signature for the adakite/high-Al TTD group is interpreted to be due to high-pressure partial melting of a basaltic source leaving a garnet amphibolite to eclogite restite assemblage, as discussed in Section 1.2. Mesozoic, Palaeozoic and Proterozoic TTD samples are also included as part of the cumulative adakite/high-Al TTD database (394 total samples). Adakite/high-Al TTD rocks range in age from the 1980 Mount St Helens dacitic volcanics (Defant & Drummond 1993) to the 3.96 Ga Acasta gneiss (Bowring *et al.* 1990).

The 13 localities used to define the Cenozoic adakite lithology (Defant & Drummond 1990) are associated with the

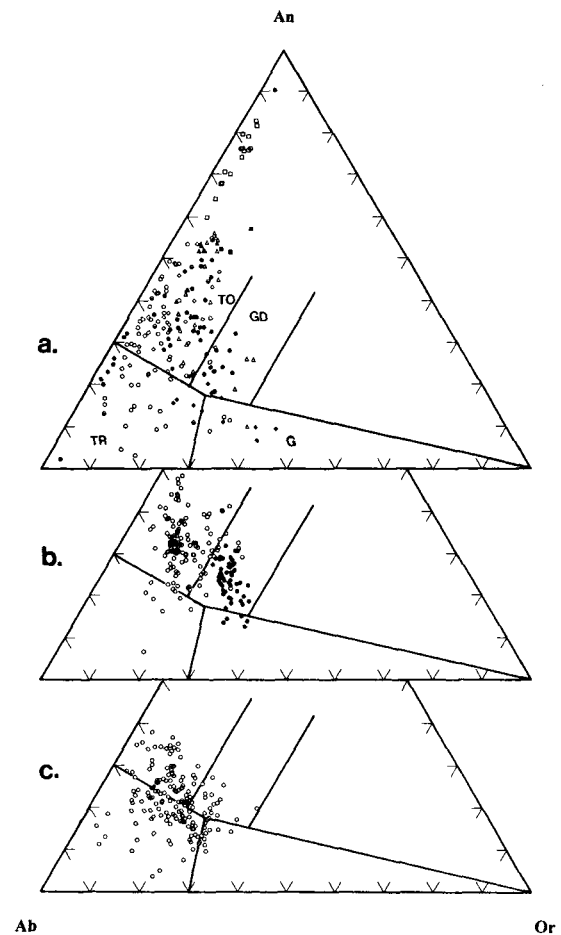


Figure 1 CIPW normative Ab–An–Or granitic rock classification after Barker (1979). TR, Trondhjemite; TO, tonalite; GD, granodiorite; and G, granite. (a) Experimental basalt partial melting data from: Holloway and Burnham (1972), closed triangle; Helz (1976), open triangle; Hacker (1990), open diamond; Rapp (1990) and Rapp *et al.* (1991), open circle; Beard & Lofgren (1991, dehydration melting only), closed circles; Rushmer (1991), closed square; Winther & Newton (1991), half-closed circle; Wolf & Wyllie (1991, 1994), open square; and Sen & Dunn (1994), closed diamond. (b) Cenozoic adakite (open circle) and CVZ/CBB (closed circle) data. (c) Archean high-Al TTD data.

subduction of oceanic lithosphere younger than 25 Ma. Parsons and Sclater (1977) found that oceanic crust younger than 25 Ma has a heat flow in the range 2.8–8.0 HFU (heat flow units), whereas older crust has a relatively constant heat flow of 1.0–2.5 HFU. We have proposed that in orogenic terranes where young, hot oceanic crust subducts, the slab has the ability to melt, producing adakite under garnet amphibolite to eclogite conditions. Numerous petrogenetic studies of Archean high-Al TTD have proposed that these magmas were also produced by high-pressure partial melting of the subducted oceanic crust (Jahn *et al.* 1981, 1984; Martin 1986, 1987, 1993; Nisbet 1987; Luais & Hawkesworth 1994). High heat flow, rapid convection and subduction of hotter, smaller oceanic plates are thought to be unique tectonic elements in the Archean which optimized conditions for the transformation of subducted oceanic crust into sial via partial melting (Abbott & Hoffman 1984; Martin 1986, 1993; Drummond & Defant 1990).

1.1. Pressure–temperature parameters for slab melting

The question of whether the subducted oceanic lithosphere directly contributes to magma production in volcanic arc terranes has provoked considerable debate since the advent of plate tectonics. One of the key issues is whether the

Table 1 Average compositional data on a variety of TTD types, arc ADR suites and boninites. ASI = alumina saturation index [(mol Al₂O₃)/(mol Na₂O + K₂O + CaO)]; Mg# = [100 • mol MgO/(mol MgO + FeO)].

| | Adakite and high-Al TTD (n=394) | Cenozoic adakite (n=140) | Archean high Al-TTD (n=174) | Continental arc ADR (n=815) | CVZ, Andes ADR (n=55) | Island arc ADR (n=473) | Low-Al TTD (n=121) | Plagiogranite (n=60) | Boninite (n=134) |
|--------------------------------|------------------------------------|-----------------------------|--------------------------------|--------------------------------|--------------------------|---------------------------|-----------------------|-------------------------|---------------------|
| SiO ₂ | 67.91 | 63.89 | 70.20 | 63.87 | 63.30 | 67.72 | 73.47 | 68.83 | 58.74 |
| TiO ₂ | 0.42 | 0.61 | 0.33 | 0.68 | 0.68 | 0.49 | 0.38 | 0.50 | 0.23 |
| Al ₂ O ₃ | 16.58 | 17.40 | 15.74 | 17.02 | 16.39 | 15.44 | 13.27 | 14.61 | 11.22 |
| FeO* | 3.03 | 4.21 | 2.56 | 4.34 | 4.84 | 4.43 | 3.40 | 4.59 | 8.53 |
| MnO | 0.06 | 0.08 | 0.04 | 0.11 | 0.08 | 0.11 | 0.22 | 0.08 | 0.17 |
| MgO | 1.53 | 2.47 | 1.09 | 2.22 | 2.37 | 1.48 | 1.16 | 1.12 | 12.09 |
| CaO | 3.89 | 5.23 | 3.17 | 4.80 | 4.58 | 3.98 | 2.54 | 3.83 | 6.77 |
| Na ₂ O | 4.77 | 4.40 | 4.87 | 4.38 | 4.11 | 3.29 | 4.45 | 5.65 | 1.69 |
| K ₂ O | 1.67 | 1.52 | 1.88 | 2.37 | 3.14 | 2.95 | 1.02 | 0.66 | 0.47 |
| P ₂ O ₅ | 0.14 | 0.19 | 0.12 | 0.21 | 0.30 | 0.11 | 0.09 | 0.13 | 0.09 |
| Sr | 668 | 869 | 495 | 424 | 730 | 229 | 133 | 150 | 100 |
| Ba | 615 | 485 | 746 | 501 | 991 | 514 | 248 | 133 | 43 |
| Rb | 41 | 30 | 50 | 83 | 91 | 109 | 20 | 15 | 11 |
| Cs | 1.95 | 1.19 | 1.73 | 9.45 | 3.42 | 0.76 | 0.78 | 0.10 | 0.49 |
| U | 0.96 | 0.99 | 1.03 | 3.61 | 3.31 | 0.67 | 0.93 | 1.42 | 0.19 |
| Th | 4.50 | 3.52 | 5.98 | 13.2 | 11.9 | 4.96 | 3.15 | 4.51 | 0.40 |
| Y | 8.8 | 9.5 | 6.8 | 27.4 | 15.0 | 28.5 | 45 | 83 | 6.1 |
| Zr | 131 | 117 | 149 | 190 | 207 | 133 | 149 | 351 | 32 |
| Hf | 3.4 | 3.5 | 3.4 | 5.5 | 5.3 | 2.6 | 4.1 | 6.6 | 1.1 |
| Nb | 6.5 | 8.3 | 5.4 | 15.0 | 9.8 | 15.8 | 4.1 | 10.4 | 2.2 |
| Ta | 0.54 | 0.53 | 0.55 | 1.17 | 1.94 | 0.49 | 0.51 | 1.87 | 0.07 |
| Sc | 7.4 | 9.1 | 4.0 | 12.1 | 8.6 | 10.9 | 13.7 | 12.3 | 33.7 |
| V | 61 | 72 | 38 | 84 | 108 | 71 | 66 | 42 | 172 |
| Cr | 38 | 54 | 36 | 29 | 25 | 21 | 12 | 21 | 969 |
| Co | 15 | 13 | 15 | 12 | 14 | 19 | 12 | 11 | 38 |
| Ni | 26 | 39 | 19 | 19 | 18 | 9 | 18 | 6 | 223 |
| Cu | 23 | 24 | 26 | 30 | 48 | 27 | 15 | 59 | 19 |
| Zn | 51 | 57 | 46 | 59 | 95 | 58 | 52 | 41 | 70 |
| La | 22.62 | 17.55 | 29.84 | 29.94 | 36.05 | 32.01 | 12.07 | 16.00 | 2.07 |
| Ce | 41.03 | 34.65 | 51.63 | 60.15 | 79.02 | 55.27 | 30.14 | 43.17 | 4.58 |
| Nd | 18.53 | 20.14 | 19.92 | 28.27 | 35.77 | 17.85 | 15.54 | 28.62 | 2.67 |
| Sm | 2.88 | 3.15 | 2.79 | 5.28 | 6.56 | 6.40 | 4.26 | 7.85 | 0.75 |
| Eu | 0.91 | 0.97 | 0.91 | 1.18 | 1.59 | 3.60 | 0.96 | 1.65 | 0.28 |
| Gd | 2.05 | 2.25 | 2.04 | 4.26 | 4.33 | 6.99 | 3.60 | 11.52 | 1.06 |
| Tb | 0.30 | 0.37 | 0.25 | 0.72 | 0.62 | 0.76 | 0.86 | 1.33 | 0.15 |
| Dy | 1.22 | 1.43 | 1.16 | 3.57 | 2.65 | 6.88 | 4.07 | 13.79 | 1.35 |
| Er | 0.64 | 0.76 | 0.59 | 2.20 | 2.65 | 5.03 | 2.76 | 9.51 | 0.90 |
| Yb | 0.65 | 0.91 | 0.46 | 2.44 | 1.22 | 4.26 | 4.03 | 7.19 | 0.89 |
| Lu | 0.11 | 0.15 | 0.09 | 0.39 | 0.17 | 0.47 | 0.65 | 1.05 | 0.15 |
| Mg# | 43 | 48 | 41 | 41 | 46 | 34 | 33 | 31 | 69 |
| ASI | 1.00 | 0.96 | 1.00 | 0.92 | 0.89 | 1.00 | 1.02 | 0.89 | 0.73 |
| Na/K | 3.87 | 3.08 | 3.08 | 2.15 | 1.18 | 1.73 | 12.9 | 90.2 | 3.89 |
| La/Sm | 8.3 | 5.4 | 12.0 | 5.1 | 5.8 | 2.3 | 2.9 | 2.0 | 2.4 |
| Sr/Y | 104 | 121 | 110 | 18 | 51 | 9.3 | 5.4 | 2.2 | 19 |
| Zr/Sm | 65 | 47 | 86 | 40 | 32 | 24 | 34 | 44 | 48 |

thermomechanical conditions of the slab can allow melting to occur. A number of studies (Wyllie 1984; Peacock 1990a, 1990b; Cloos 1993; Peacock *et al.* 1994) have shown that slab melting is possible under a restricted set of conditions: (1) a young, hot subducting slab; (2) initiation of subduction providing a pristine, warm mantle wedge setting; or (3) the presence of high shear stresses in the subduction zone associated with highly oblique convergence and/or slow subduction. The original adakite localities of Defant and Drummond (1990) were attributed to melting young, hot subducting slab material. Three new adakite localities are associated with the subduction of young, hot oceanic crust: Late Miocene Cerro Pampa andesites–dacites, southern Argentina (Kay *et al.* 1993), Quaternary volcanic rocks of the Cordillera de Talamanca, Costa Rica (Drummond *et al.* 1995) and Quaternary volcanic rocks of SW Japan (Morris 1995). On the other hand, the initiation of subduction and high shear stress are interpreted causes for adakite generation from new localities in Mindanao, Philippines (Sajona *et al.* 1993) and the western Aleutians (Yogodzinski *et al.* 1995), respectively.

Figure 2 illustrates a slab geotherm of $10^{\circ}\text{C km}^{-1}$ which would correspond to the special conditions required for slab melting. In addition, a $10^{\circ}\text{C km}^{-1}$ geotherm correlates with many natural P – T estimates from exhumed subduction zone material, such as: (1) the top of the slab geotherm measured from the Zagros Mountains (Bird *et al.* 1975); (2) the P – T field recorded by subduction-related (type C) eclogites (Raheim & Green 1975); and (3) the P – T conditions from the Betic ophiolite, Spain (650–700°C, 20 kbar; Puga *et al.* 1995), Tauern window eclogites, Austria (625°C, 20 kbar; Selverstone *et al.* 1992), Monviso ophiolite, western Alps (500±50°C, 10–11 kbar, Philippot & Selverstone 1991) and the Adula nappe, central Alps (500–820°C, 17–27 kbar; Droop *et al.* 1990), among others.

Partial melting of the slab would require a source of water from dehydration reactions given the unrealistic thermal requirements for the dry melting of basalt (curve 11, Fig. 2). Thus the wet basalt solidus (curve 10; Green 1982) provides the minimum thermal conditions for slab melting. Under typical arc conditions the slab is thought to dehydrate, contributing fluids to the overlying mantle wedge that initiates melting of the mantle and BADR (basalt–andesite–dacite–rhyolite) arc volcanic production (see Tatsumi & Eggins 1995

and references cited therein). Slab dehydration is a continuous and progressive process that may be tracked by a series of dehydration reactions. Figure 2 indicates that numerous potential dehydration reactions correspond to the P – T conditions of the wet basalt solidus and the 10°C/km geotherm. In addition to these potential slab dehydration reactions, serpentinised subducted oceanic mantle could provide a major source of water to the subduction system. Ulmer and Trommsdorff (1995) have shown experimentally that antigorite breaks down to forsterite+enstatite+H₂O at 25 kbar and 730°C, having the capacity to release up to 13 wt% water. If these potential dehydration fluids experience significant residence time in the slab under super-solidus conditions, then partial melting is an obvious consequence.

In combination with the 10°C/km slab geotherm and wet basalt solidus, the hornblende dehydration curve (curve 1) envelops a P – T regime (700–800°C, 22–26 kbar) that would correspond to slab melting under garnet amphibolite to hornblende eclogite conditions. At P – T conditions below minimum basalt partial melting (650°C and 22 kbar), Poli (1993) experimentally confirmed the presence of hornblende eclogite as the stable metamorphic lithology. Drummond and Defant (1990) call on the retention of hornblende at the site of partial melting to explain many of the adakite geochemical features (e.g. high Al₂O₃, low K/Rb and Nb). Garnet is a key restite phase to generate the low HREE, Y and Sc contents of the adakites (Table 1); thus minimum P – T conditions must correspond to garnet stability during basalt partial melting. The present consensus from experimental work has shown that P – T conditions of ≥ 15 kbar and $\geq 750^{\circ}\text{C}$ are required to generate TTD with the requisite major and trace element character of adakite/high-Al TTD in the presence of a garnet amphibolite to eclogite refractory assemblage (Rapp *et al.* 1991; Winther & Newton 1991; Rushmer *et al.* 1994; Sen & Dunn 1994; Thompson & Ellis 1994). Thompson and Ellis (1994) favour a P – T regime of 800°C and 26 kbar for partial dehydration melting of a basaltic source following the reaction: zoisite + hornblende + quartz = clinopyroxene + pyrope + high-Al TTD melt.

The question remains, however, whether the dehydration fluids residence time in the slab is sufficient to initiate partial melting. Drummond and Defant (1990) speculated that dehydration fluids associated with slab melting would be largely retained in the slab and involve intraslab migration. This problem has been studied in exhumed subduction zone complexes from the Monviso ophiolite (Philippot & Selverstone 1991) and Tauern window (Selverstone *et al.* 1992). These studies have found that during eclogitisation of the subducted slab only localised, limited fluid flow and metasomatism occur under subsolidus conditions. Tauern window eclogites demonstrate that isolated fluid-filled pockets can exist at 20 kbar, giving rise to clinozoisite–zoisite–phengite–rutile segregations under transient $P_{\text{fluid}} = P_{\text{total}}$ conditions. Metamorphic fluid studies in the exhumed eclogitic slabs indicate that at depths of $> 50 \pm 10$ km the slab retains its dehydration fluid (Selverstone *et al.* 1992; Philippot 1993), limiting fluid migration to intraslab fluid flow. In a preserved subduction complex that has experienced partial melting of the amphibolitic to eclogitic MORB, such as the Catalina Schist terrane, pervasive fluid flow involved metasomatism of the mantle wedge (Sørensen 1988; Sørensen & Grossman 1989). This suggests that transfer of fluids from the slab into the mantle wedge at depths $> 50 \pm 10$ km is facilitated by slab melting. Philippot (1993) further suggests that all deep transfer of water into the mantle is by a water-rich melt phase.

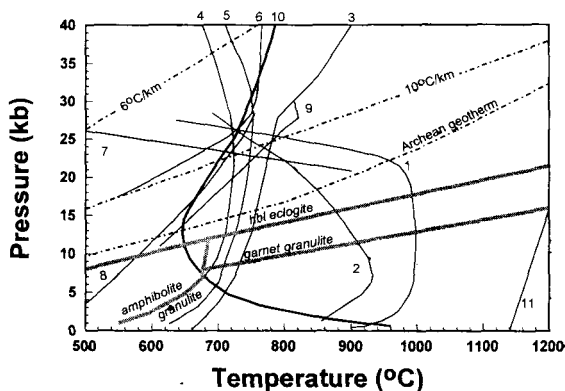


Figure 2 P – T diagram depicting potential slab melt conditions in concert with dehydration reactions. Pertinent curves include: (1) hornblende-out (Wyllie 1982); (2) tremolite-out (Obata & Thompson 1981); (3) biotite-out (Tatsumi & Eggins 1995); (4) serpentine-out (Tatsumi & Nakamura 1986); (5) talc-out (Wyllie 1982); (6) Mg–chloritoid-out (Schreyer 1988); (7) paragonite-out (Holland 1979); (8) clinochamite-out (Engi & Lindsley 1980); (9) talc + phengite-out (Massone & Schreyer 1989); (10) and (11) wet (Green 1982) and dry (Wyllie 1982) basalt solidus, respectively; Archaean geotherm (Martin 1993); and metamorphic facies fields (Cloos 1993).

1.2. Geochemical parameters for slab melting

Figure 1b and 1c indicate that the Cenozoic adakites and Archean high-Al TTD data fall primarily within the trondhjemite, tonalite and granodiorite fields, corresponding to the compositional spread of experimental melts (Fig. 1a) from basaltic sources. Comparison between Cenozoic adakite and Archean high-Al TTD (Table 1, Fig. 1b, 1c) indicates that the Cenozoic adakites are relatively less felsic with a higher An proportion + ferromagnesian component + trace transition metal content and lower SiO₂. However, both groups exhibit low Y, Yb and Sc values indicative of a garnet-bearing residue at the site of basalt partial melting and are considered as a coherent petrogenetic group, i.e. high-pressure partial melting of a basaltic source.

Arth (1979) proposed a subdivision of TTD on the basis of Al₂O₃-Yb relationship (Fig. 3). Removal of subaluminous hornblende and garnet either as restite components or early crystallisation phases under high pressure conditions produces the low Yb-high Al₂O₃ character of adakite/high-Al TTD (Fig. 3). Trace element modelling (Kay 1978; Jahn *et al.* 1981; Martin 1986; Drummond & Defant 1990) has shown that the low Yb_N and high (La/Yb)_N of adakite/high-Al TTD is due to a garnet amphibolite to eclogite restite assemblage. Low-Al TTD, island arc ADRs and plagiogranites exhibit a high Yb content (cumulatively referred to as the high-Yb TTD group) due to plagioclase + pyroxene extraction on partial melting and/or differentiation at low pressures (Drummond & Defant 1990; Beard 1995). The low-Al TTD has low Al₂O₃ and Sr values (Table 1) due to dominant plagioclase removal. Mantle-derived boninites define their own unique field with low Al₂O₃ and Yb. The overlap between adakite/high-Al TTD and specific continental ADR samples in Figure 3 is addressed in Section 2.

Y-Sr/Y relationships closely track the influence of garnet and plagioclase in TTD genesis (Drummond & Defant 1990; Defant & Drummond 1990). Strontium behaves incompatibly on high-pressure partial melting of basalt due to the absence or instability of plagioclase, whereas Y is dominantly controlled by the garnet fraction in the restite. Cenozoic adakites and Archean high-Al TTD samples are plotted on Figure 4 with respect to two partial melting models. The two models involve two basaltic source compositions, an Archean mafic composite (AMC; Drummond & Defant 1990) and an average MORB (Gill 1981), which experience 10–50% partial melting leaving either 10% garnet amphibolite and eclogite restite assemblages. The AMC and MORB partial melting models correspond well with the Archean high-Al TTD and Cenozoic adakite data, respectively. Independent analyses of Y-Sr/Y relationships with slab melting corroborate the model of adakite generation

by 10–50% partial melting of a MORB source under eclogitic to hornblende eclogitic conditions (Tsuchiya & Kanisawa 1994). The high-Yb TTD group (Fig. 3) display a high Y, low Sr/Y content (shaded area, Fig. 4) due to the incompatible and compatible behaviour of Y and Sr, respectively, associated with a dominant plagioclase-pyroxene extract assemblage.

A plot of La/Sm versus Zr/Sm (Fig. 5) subdivides the adakite/high-Al TTD group from the high-Yb TTD group and boninites at a La/Sm ratio of four. The high La/Sm reflects the strong affinity of garnet and hornblende for Sm relative to La. Partial melting (1–50%) curves of MORB leaving a 10% garnet amphibolite (upper curve) and eclogite (lower curve) are shown on Figure 5. Although the adakite/high-Al TTD exhibits a range of Zr/Sm, many (40% of the samples) display elevated values of Zr/Sm > 60. Pearce and co-workers (Pearce *et al.* 1992; Pearce & Peate 1995) have suggested that Zr behaves non-conservatively during slab melting due to the incompatibility of Zr in residual hornblende, which may explain the elevated Zr/Sm for some adakite/high-Al TTD under garnet amphibolitic melting conditions.

Optimum conditions for TTD melt segregation from a garnet- and hornblende-bearing basaltic protolith occur at 20–30% melting (Rapp 1995); however, above hornblende-out conditions the melt percentage increases to 50%, producing a

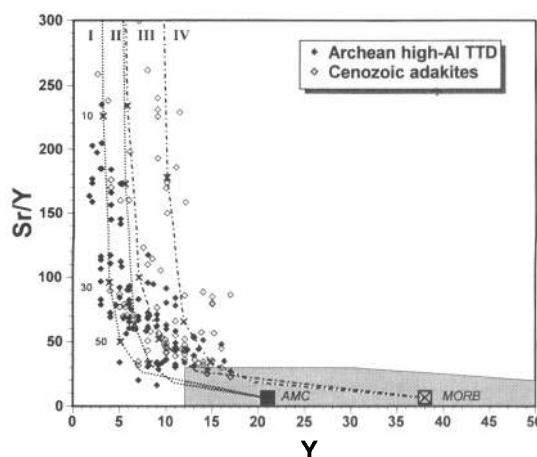


Figure 4 Y (ppm)-Sr/Y diagram with Archean high-Al TTD and Cenozoic adakites plotted relative to partial melt curves of MORB (values of Gill 1981) and Archean mafic composite (AMC values of Drummond & Defant 1990) sources leaving either eclogite (curves I and III) or 10% garnet amphibolite (curves II and IV) restite. Percentage partial melt values are labelled at the X on curve. High-Yb TTD group field is shaded.

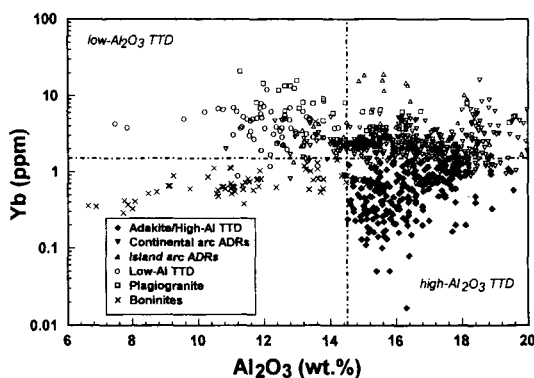


Figure 3 Al₂O₃ (wt.%)–Yb (ppm) plot of various TTD types and boninites with high-Al₂O₃ and low-Al₂O₃ TTD subdivision of Arth (1979).

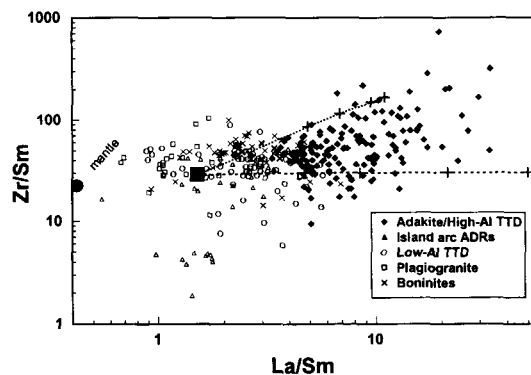


Figure 5 La/Sm–Zr/Sm plot of TTD types and boninites relative to partial melt curves of MORB (closed square) leaving either a 10% garnet amphibolite (upper curve) or eclogite (lower curve) restite. Percentage partial melt values are shown with a cross (+) and represent 1, 10, 30 and 50% melt with decreasing La/Sm. Mantle value from Hole *et al.* (1984).

more metaluminous, intermediate melt composition (Rapp & Watson 1995). Adakite/high-Al TTD samples that correspond to $\approx 50\%$ partial melting on Figures 4 and 5 may be the result of hornblende decomposition or the addition of a minor mantle component (Section 3).

2. Slab melting versus lower crustal melting comparison

An alternative hypothesis to slab melting for high-Al TTD/adakite genesis involves the partial melting of overthickened continental arc crust (Kay & Kay 1991, 1993; Atherton & Petford 1993). In fact, some continental arc ADR localities, such as those in the central volcanic zone, Andes (CVZ), possess high La/Yb and Sr/Y ratios (Kay & Kay 1991, 1993; Feeley & Hacker 1995). To compare adakite compositions against ADR from overthickened continental arc terranes, 55 samples from the CVZ (Nevados de Payachata volcanic region—Davidson *et al.* 1990; volcan Tata Sabaya—de Silva *et al.* 1993; volcan Ollague—Feeley & Davidson 1994; Feeley & Hacker 1995) and from the Cordillera Blanca batholith (CBB), Peru (Atherton & Sanderson 1987) are used (average shown in Table 1). In addition, partial K_2O –Rb–Sr isotopic data (Harmon *et al.* 1984) from the CVZ is also used for comparative purposes. The Quaternary volcanic rocks of the CVZ and the 5–7 Ma volcanic and plutonic rocks of the CBB correspond to a crustal thicknesses of 60–70 km and 50 km, respectively.

Continental arc ADR data from arcs of normal crustal thickness (e.g. 30–40 km) exhibit elevated Cs and U values relative to adakite/high-Al TTD due to the incorporation of or derivation from continental crust (Table 1). Figure 6 displays the high Y and Cs values of the continental arc ADRs indicative of a garnet-free crustal signature. However, the CVZ/CBB and Cenozoic adakite data compositionally overlap at low Y–Cs values (Fig. 6). The low Y and Yb values of the CVZ/CBB are attributed to one of the following models: (1) direct partial melting of a garnet-bearing mafic lower crustal source in the case of the CBB (Atherton & Petford 1993); (2) AFC of mantle-derived basaltic parental magmas with garnet-bearing lower crust for volcan Ollague, CVZ (Feeley & Hacker 1995); or (3) mixing of mantle-derived normal arc magmas with lower crustal melts in the Nevados de Payachata volcanic region, CVZ (Davidson *et al.* 1990). Atherton and Petford (1993) and Feeley and Hacker (1995) further suggest that adakites should be re-evaluated relative to their petrogenetic models for the CVZ/CBB.

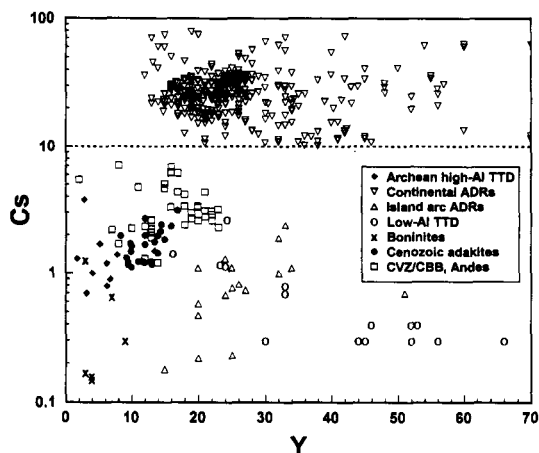


Figure 6 Y (ppm)–Cs (ppm) diagram of TTD types, boninites and CVZ/CBB Andes data.

Adakites have a low Sr isotopic character (Kay 1978; Defant *et al.* 1992; Kay *et al.* 1993). The adakites of Panama and Costa Rica have some of the lowest radiogenic isotopic ratios of any Central American arc volcanic rocks (Defant *et al.* 1992). In the modern central and eastern Aleutians only the Adak Island adakites contain a MORB-like isotopic signature (Kay 1978; Yogodzinski *et al.* 1994). The CVZ volcanic rocks, on the other hand, are noted for their elevated Sr and O isotopic signature resulting from a lower continental crustal component (Harmon *et al.* 1984). A clean separation exists between adakite and CVZ/CBB Sr isotopic data at a Sr isotopic value of 0.7045 (Fig. 7a, 7b). Although some K_2O and Rb overlap occurs between the two data sets, the CVZ/CBB data are generally more K_2O - and Rb-enriched (Fig. 7a, 7b). Comparison of average K_2O , Rb and Na/K between adakite and CVZ/CBB (Table 1) indicates the more potassic character of the CVZ/CBB samples. As stated earlier, slab melts should reside primarily within the trondhjemite–tonalite fields (Fig. 1). The CVZ/CBB data fall consistently within the granodiorite–granite fields (Fig. 1c), which argues against a MORB source. Therefore, magmas derived from or mixed with a lower crustal component in overthickened (> 50 km) arc terranes may exhibit some adakite-like compositional characteristics due to the influence of garnet and hornblende stability; however, close scrutiny of Sr isotopes in combination with the K_2O and Rb content should discriminate between slab melting and a lower crustal derivation.

3. Adakite–mantle interaction

Emplacement of adakitic magmas from the slab into the overlying continental or island arc crust requires ascent through the mantle wedge. The degree to which adakite magmas and the mantle interact is dependent on many factors, such as the ascent rate, subduction angle, slab geotherm and

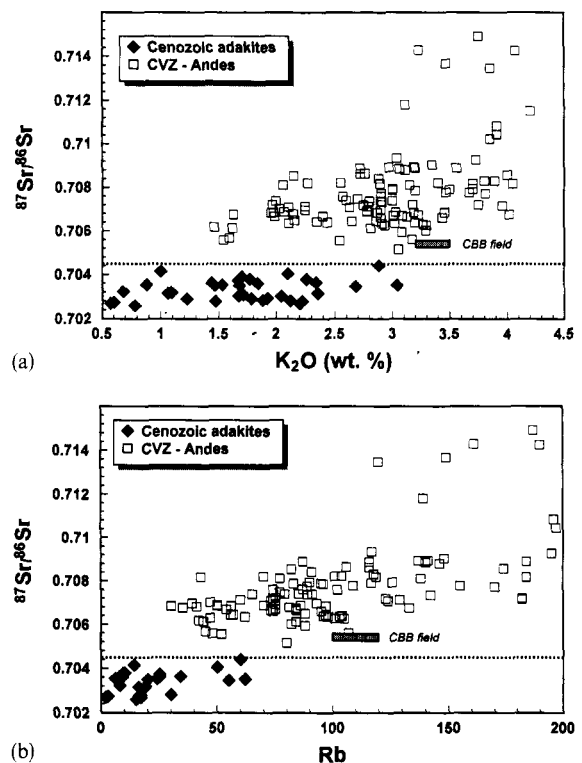


Figure 7 (a) K_2O (wt.%)– $^{87}Sr/^{86}Sr$ plot of Cenozoic adakites versus CVZ and CBB (shaded field), Andes data. CBB field represents range of values reported by Atherton & Sanderson (1987) and Atherton & Petford (1993). (b) Rb (ppm)– $^{87}Sr/^{86}Sr$ plot of Cenozoic adakites versus CVZ and CBB (shaded field), Andes data.

depth of melting, thickness of the overriding lithosphere and the amount of prior adakite–mantle reaction within a ascent conduit. Beard *et al.* (1993) state ‘that slab melts should show some evidence of equilibration (or, at least, reaction) with mantle peridotite during ascent’ and chemical quantification of this process would aid in further defining adakites as a unique lithology.

Experimental studies of TTD melt–peridotite reactions at elevated pressures (15–30 kbar) have shown that the melt will react with peridotite producing orthopyroxene ± garnet ± hornblende ± clinopyroxene in the metasomatised peridotite (Carroll & Wyllie 1989; Johnston & Wyllie 1989; Sen & Dunn 1995). The dominant reaction involves melt + olivine ± clinopyroxene reacting to orthopyroxene ± hornblende. Sen and Dunn (1995) indicate that mantle metasomatism will initially produce hornblende-bearing harzburgite followed by hornblende-bearing orthopyroxenite production. The TTD melt would become more CaO- and MgO-enriched until it becomes saturated with respect to the metasomatic phases, whereupon further reaction/assimilation would simply cause additional reactant phase(s) precipitation and ultimate melt consumption (Carroll & Wyllie 1989; Johnston & Wyllie 1989).

Recent work by Yogodzinski and co-workers (1994, 1995) in the western Aleutians has evaluated geochemically the effects of slab melt–mantle interaction in a volcanic arc setting. They define two high-Mg andesite (HMA) types: Piip-type and Adak-type. Piip-type HMA is interpreted to represent volcanic rocks from a enriched peridotite source that was generated by mixing depleted MORB mantle with minor (~4%) adakite melts. The HMAs from the Setouchi belt, SW Japan (Tatsumi & Ishizaka 1982) were included into the Piip-type category (Yogodzinski *et al.* 1994). The Adak-type HMA, which we refer to as transitional adakites, represent CaO- and MgO-rich adakites from the western Aleutians, Adak Island–central Aleutians (Kay 1978), the Austral Andes (Stern *et al.* 1984) and Baja California (Saunders *et al.* 1987) and are produced as slab melts that incompletely interacted with the mantle wedge on ascent (Kay 1978; Yogodzinski *et al.* 1995).

A Cr–Ni plot (Fig. 8) demonstrates the relationship between adakites, transitional adakites, Piip-type HMAs and boninites. Partial melting of average mantle (Frey *et al.* 1978) leaving either a garnet peridotite or harzburgite residuum generates model curves that closely coincide with the boninite samples

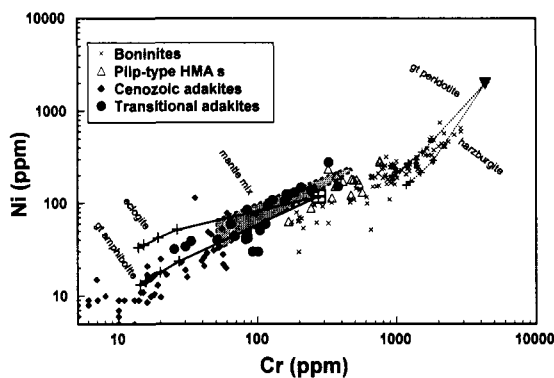


Figure 8 Cr (ppm)–Ni (ppm) diagram with MORB (square with cross) partial melting curves leaving 10% garnet amphibolite and eclogite restite. Mantle (Frey *et al.* 1978) partial melt curves on both garnet peridotite (olivine₆₀orthopyroxene₂₀clinopyroxene₁₀garnet₁₀ peridotite of Mysen 1982) and harzburgite (olivine₈₀orthopyroxene₂₀) stability fields. Percentage partial melt values are depicted by a cross (+) on curves and represent 1, 10, 30 and 50% partial melt with increasing Ni and Cr values. Shaded mantle mix box represents 1–10% mix of mantle component into 1–50% MORB partial melt component.

and produces a Cr:Ni ratio of 4:1 to 5:1. Melting a MORB source under eclogitic to garnet amphibolitic conditions produces model curves with lower Cr:Ni ratios of 1.5:1 to 2:1, which corresponds to the low Cr:Ni ratios of adakite. A mixture of mantle and modelled slab melt compositions yields a mantle mix region (1–10% mantle component, Fig. 8) that coincides with many of the transitional adakite samples. The low Cr:Ni ratio of adakites and transitional adakites may be attributed to the strong affinity of restitic garnet–hornblende–clinopyroxene for Cr relative to Ni. Comparison between transitional adakites and boninites at comparable Ni values indicates that the transitional adakites are 100–200 ppm deficient in Cr, which is partially due to the relatively low Cr values of the initial slab melt. In addition, the reaction between adakite and mantle decomposes olivine, liberating Ni and Cr, with Cr being preferentially accepted in the metasomatic assemblage of orthopyroxene, hornblende and garnet. Most of the Piip-type HMAs display higher Cr values than the transitional adakites, which is consistent with a more dominant mantle source with minor slab melt component. Type-area boninites (Chichijima, Bonin Islands) may also have a minor (2%) slab melt component in the mantle source to explain their high Zr/Sm ratios (~60) (Taylor *et al.* 1994). The minor overlap between Piip-type HMAs and some boninites may be due to a common petrogenesis.

Major element relationships, such as MgO–SiO₂ (Fig. 9), between adakites, transitional adakites, Piip-type HMAs and boninites supports minor mantle–slab melt interaction for the transitional adakites and adakite-contaminated mantle source for the Piip-type HMAs. Transitional adakites fall within the mantle mix region (1–10% mantle component), whereas the Piip-type HMAs are generally more enriched in MgO than the transitional adakites. Kelemen (1995), in a review of HMA geochemistry, concludes that HMA genesis is best explained by silicate melt–peridotite reaction. In this study, Kelemen states that a reaction between felsic slab melt and mantle peridotite will cause a sharp increase in the MgO and Ni content of the melt due to olivine dissolution and/or reaction-out to orthopyroxene. Our observations on Ni (Fig. 8) and MgO (Fig. 9) behaviour during adakite–mantle reaction agree with those of Kelemen (1995). An additional lithology shown on Figure 9 is commonly temporally and spatially related to adakites, Nb-enriched arc basalts (NEAB) (Defant *et al.* 1992), and delineates a continuous trend with the adakites and transitional adakites. The unusual composition of NEAB is apparently influenced by slab melting and adakite–mantle mixing (Section 3.1).

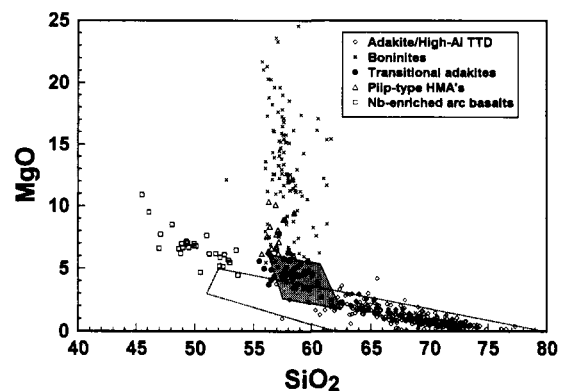


Figure 9 SiO₂ (wt%)–MgO (wt%) plot with experimental basalt partial melts (open field, see Fig. 1 for data sources) and 1–10% mantle (pyrolite of Ringwood 1975)–slab melt mix region (shaded field) shown relative to adakite-types, boninites and NEABs.

3.1. Case example of adakite–mantle interaction: northern Kamchatka, Russia

Our studies have focused on the northern Kamchatka adakites (Kepezhinskas 1989; Defant & Drummond 1990; Hochstaedter *et al.* 1994) and interaction of the slab melts with the sub-arc mantle. Adakites are found in two northern Kamchatka localities, the Tymlat volcanic field (Kepezhinskas 1989; Defant & Drummond 1990) and the Valovayam volcanic field (Hochstaedter *et al.* 1994). Adakite generation is interpreted to be associated with the subduction of young (< 15 Ma), hot Komandorsky basin oceanic crust that apparently ceased about 2 Ma (Kepezhinskas 1989; Hochstaedter *et al.* 1994). Contemporaneous Nb-enriched arc basalts (7 Ma) occur with transitional adakites (6–8 Ma) in Valovayam as interlayered flows or as individual cinder cones or dykes in the vicinity of the transitional adakites (Hochstaedter *et al.* 1994; Kepezhinskas *et al.* in press).

The Valovayam NEABs host a suite of mantle xenoliths (dunites, websterites, spinel lherzolites, amphibole wehrlites, spinel pyroxenites, amphibole pyroxenites and garnet pyroxenites) that have experienced various degrees of Na metasomatism (Kepezhinskas *et al.* 1995). A metasomatic assemblage of Cr-poor, Al–Fe–Mg and Al–Ti–Fe spinel, Al-rich (up to 10 wt% Al₂O₃) augite, Cr-diopside, high-Al and Na pargasitic amphibole and almandine–grossularite garnet is found replacing mantle olivine and pyroxene (Kepezhinskas *et al.* 1995). In addition, andesine megacrysts occur in the host NEAB due to Na-metasomatic effects. The metasomatic assemblage is similar to that predicted from TTD melt–peridotite reactions from experimental studies (Carroll & Wyllie 1989; Sen & Dunn 1995), with the exception of lacking orthopyroxene.

Metasomatism of these mantle xenoliths requires the addition of Si, Al and Na, which may be introduced from a adakitic melt phase. Kepezhinskas *et al.* (1995) have suggested that trondhjemitic veinlets found in some of the Valovayam mantle xenoliths are the metasomatising agents. The trondhjemitic veinlets are comprised of felsic glass (SiO₂ = 63.88 wt%) with hornblende + plagioclase + magnetite. The glass has high Na/K (5.45), Sr (1736 ppm), La/Sm (8.0), La/Yb (22.8) and Sr/Y (289) and low Y (6 ppm), which is characteristic of adakite compositions (Kepezhinskas *et al.* 1996). However, the high Cr (349 ppm) and Yb (2.92 ppm) content in the trondhjemitic glass suggests that reaction and selective contamination with mantle components has occurred in the veinlets. The trace element chemistry of the mantle clinopyroxenes indicates an increase in Na and Al with increasing Sr, La/Yb and Zr/Sm, which is attributed to reaction with an adakite melt component (Kepezhinskas *et al.* 1996).

A model for adakite–transitional adakite–Na metasomatism of the sub-arc mantle in northern Kamchatka would include: (1) partial melting of the slab at 75–85 km depth; (2) ascent of adakite into overlying mantle; (3) adakite–peridotite interaction; and (4) melting of Na-metasomatised mantle to produce NEAB magmas that host the cognate mantle xenoliths (Kepezhinskas *et al.* 1995, 1996). The lithological association of adakite–transitional adakite–Piip-type HMA–NEAB is interpreted to represent the progressive interaction between slab melts and sub-arc mantle.

4. Conclusions

Trondhjemite–tonalite–dacite magmas (high-Al TTD/adakite) with a unique compositional character can be generated by high-pressure partial melting of a basaltic source under garnet amphibolite to eclogitic conditions. Under the elevated geotherms of the Archean, the production of high-Al TTD is

considered to be a major continental crust forming mechanism (Martin 1993). In Cenozoic tectonic regimes where young, hot oceanic crust has subducted, melting of the subducted slab can occur. We consider the approximate upper age limit for slab melt generation to be 25 Ma, primarily on the basis of natural occurrences of adakite localities (Drummond & Defant 1990; Defant & Drummond 1990). However, melting of older oceanic lithosphere is found in tectonic settings associated with oblique subduction and attendant high shear stresses (Yogodzinski *et al.* 1995) and incipient subduction into warm, pristine mantle wedge material (Sajona *et al.* 1993). Magnetic lineation maps of the world's ocean basins (Cande *et al.* 1989) indicates that approximately 20% of the ocean floor is comprised of Miocene or younger crust, which implies that adakite generation may not be as rare as originally thought.

Intermediate to felsic arc volcanic and plutonic rocks from an overthickened continental arc (CVZ/CBB, Andes) setting have some compositional similarities with adakites (e.g. high Sr/Y and La/Yb) due to plagioclase instability and involvement of garnet in their petrogenesis. However, adakite compositions can be differentiated from CVZ/CBB data on the basis of lower Sr isotopic composition, lower large ion lithophile element concentrations (Fig. 10), positive Sr anomaly and common presence of a mantle component (MgO, Cr and Ni) in the slab melts (Fig. 10). Adakites and transitional adakites show progressive enrichment in Cr and Ni content due to mantle contamination. The positive Ni anomaly (Fig. 10) is interpreted to result from the affinity of Cr for both restite phases and metasomatic phases at the site of partial melting and melt–mantle interaction, respectively, relative to Ni.

In conclusion, progress has been made on three fronts: (1) categorisation of the physical, tectonic and geochemical parameters of slab melting has been more narrowly defined; (2) discrimination between lower crustal and slab melt geochemistries is possible; and (3) the geochemical signature imparted on a adakite magma by the mantle wedge (and vice versa) is recognised.

Acknowledgements

We acknowledge NSF grants EAR-9103062 and EAR-9401931 for support of our past and present research in Kamchatka. Alfred Hochstaedter has been a valuable member of our Kamchatka research team and we give thanks for his work on this project. Discussions with Jim Beard, George DeVore and the numerous participants in the 1992 Penrose Conference on 'Origin and emplacement of low-K silicic magmas in subduction settings' have contributed to our understanding of

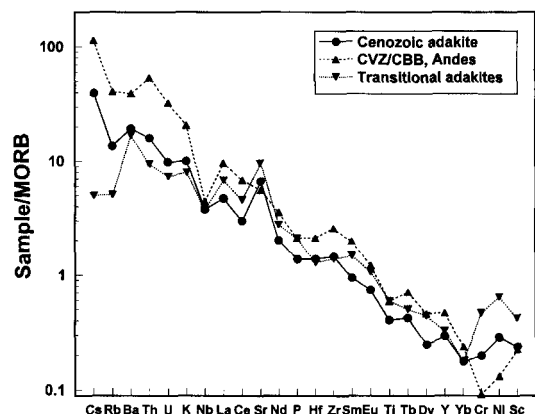


Figure 10 Multi-element variation diagram of average Cenozoic adakite, CVZ/CBB Andes (Table 1) and transitional adakite. MORB normalizing values of Taylor and McLennan (1985).

TTD magmas. Journal reviews of Mike Atherton, Jim Beard and Bob Kay are warmly appreciated.

6. References

- Abbott, D. H. & Hoffman, S. E. 1984. Archaean plate tectonics revisited 1. Heat flow, spreading rate, and the age of subducting oceanic lithosphere and their effects on the origin and evolution of continents. *TECTONICS* **3**, 429–48.
- Arculus, R. J. & Powell, R. 1986. Source component mixing in the regions of arc magma generation. *J GEOPHYS RES* **91**, 5913–26.
- Armstrong, R. L. 1981. Radiogenic isotopes: the case for crustal recycling on a near-steady-state no-continental-growth Earth. *PHIL TRANS R SOC LONDON A301*, 443–72.
- Arth, J. G. 1979. Some trace elements in trondhjemites—their implications to magma genesis and paleotectonic setting. In Barker, F. (ed.) *Trondhjemites, dacites, and related rocks*, 123–132. New York: Elsevier.
- Atherton, M. P. & Petford, N. 1993. Generation of sodium-rich magmas from newly underplated basaltic crust. *NATURE* **362**, 144–6.
- Atherton, M. P. & Sanderson, L. M. 1987. The Cordillera Blanca Batholith: a study of granite intrusion and the relation of crustal thickening to peraluminosity. *GEOL RUNDSCH* **76**, 213–32.
- Barker, F. 1979. Trondhjemite: definition, environment and hypotheses or origin. In Barker, F. (ed.) *Trondhjemites, dacites, and related rocks*, 1–12. New York: Elsevier.
- Barker, F., Arth, J. G., Peterman, Z. E. & Friedman, I. 1976. The 1.7- to 1.8-b.y.-old trondhjemites of southwestern Colorado and northern New Mexico. *GEOL SOC AM BULL* **87**, 189–98.
- Beard, J. S. 1995. Experimental, geological, and geochemical constraints on the origins of low-K silicic magmas in oceanic arcs. *J GEOPHYS RES* **100**, 15 593–600.
- Beard, J. S. & Lofgren, G. E. 1991. Dehydration melting and water-saturated melting of basaltic and andesitic greenstones and amphibolites at 1, 3, and 6.9 kb. *J PETROL* **32**, 365–401.
- Beard, J. S., Bergantz, G. W., Defant, M. J. & Drummond, M. S. 1993. Origin and emplacement of low-K silicic magmas in subduction setting: Penrose Conference Report. *GSA TODAY* **3**, 38.
- Bird, P., Toksov, M. N. & Sleep, N. H. 1975. Thermal and mechanical models of continent–continent convergence zones. *J GEOPHYS RES* **80**, 4405–16.
- Bowring, S. A., Housh, T. B. & Isachsen, C. E. 1990. The Acasta gneisses: remnant of earth's early crust. In Newsom, H. E. & Jones, J. H. (ed.) *Origin of the earth*, 319–43. New York: Oxford.
- Cande, S. C., LaBreque, J. L., Larson, R. L., Pitman, W. C., Golovchenko, X. & Haxby, W. F. 1989. *Magnetic lineations of the world's ocean basins*. Tulsa: American Association of Petroleum Geologists.
- Carroll, M. R. & Wyllie, P. J. 1989. Experimental phase relations in the system tonalite–peridotite–H₂O at 15 kb; implications for assimilation and differentiation processes near the crust–mantle boundary. *J PETROL* **30**, 1351–82.
- Cloos, M. 1993. Lithospheric buoyancy and collisional orogenesis: subduction of oceanic plateaus, continental margins, island arcs, spreading ridges, and seamounts. *GEOL SOC AM BULL* **105**, 715–37.
- Condie, K. C. 1981. *Archean greenstone belts*. New York: Elsevier.
- Davidson, J. P., McMillan, N. J., Moorbath, S., Worner, G., Harmon, R. S. & Lopez-Escobar, L. 1990. The Nevados de Payachata volcanic region (18°S/69°W, N. Chile) II. Evidence for widespread crustal involvement in Andean magmatism. *CONTRIB MINERAL PETROL* **105**, 412–32.
- Defant, M. J. & Drummond, M. S. 1990. Derivation of some modern arc magmas by melting of young subducted lithosphere. *NATURE* **347**, 662–5.
- Defant, M. J. & Drummond, M. S. 1993. Mount St. Helens: potential example of the partial melting of the subducted lithosphere in a volcanic arc. *GEOLOGY* **21**, 547–50.
- Defant, M. J., Jackson, T. E., Drummond, M. S., de Boer, J. Z., Bellon, H., Feigenson, M. D., Maury, R. C. & Stewart, R. H. 1992. The geochemistry of young volcanism throughout western Panama and southeastern Costa Rica: an overview. *J GEOL SOC LONDON* **149**, 569–79.
- de Silva, S. L., Davidson, J. P., Croudace, I. W. & Escobar, A. 1993. Volcanological and petrological evolution of Volcan Tata Sabaya, SW Bolivia. *J VOLCANOL GEOTHERM RES* **55**, 305–35.
- Dewey, J. F. & Windley, B. F. 1981. Growth and differentiation of the continental crust. *PHIL TRANS R SOC LONDON A301*, 189–206.
- Droop, G. T. R., Lombardo, B. & Pognante, U. 1990. Formation and distribution of eclogite facies rocks in the Alps. In Carswell, D. A. (ed.) *Eclogite facies rocks*, 225–59. New York: Chapman & Hall.
- Drummond, M. S. & Defant, M. J. 1990. A model for trondhjemite–tonalite–dacite genesis and crustal growth via slab melting: Archean to modern comparisons. *J GEOPHYS RES* **95**, 21 503–521.
- Drummond, M. S., Bordelon, M., de Boer, J. Z., Defant, M. J., Bellon, H. & Feigenson, M. D. 1995. Igneous petrogenesis and tectonic setting of plutonic and volcanic rocks of the Cordillera de Talamanca, Costa Rica—Panama, Central American arc. *AM J SCI* **295**, 875–919.
- Ellam, R. M. & Hawkesworth, C. J. 1988. Elemental and isotopic variations in subduction related basalts: evidence for a three component model. *CONTRIB MINERAL PETROL* **98**, 72–80.
- Engi, M. & Lindsley, D. H. 1980. Stability of titanium clinohumite: experiments and thermodynamic analyses. *CONTRIB MINERAL PETROL* **72**, 415–24.
- Feeley, T. C. & Davidson, J. P. 1994. Petrology of calc-alkaline lavas at Volcan Ollague and the origin of compositional diversity at central Andean stratovolcanoes. *J PETROL* **35**, 1295–340.
- Feeley, T. C. & Hacker, M. D. 1995. Intracrustal derivation of Na-rich andesitic and dacitic magmas: an example from Volcan Ollague, Andean Central Volcanic zone. *J GEOL* **103**, 213–25.
- Frey, F. A., Green, D. H. & Roy, S. 1978. Integrated models of basalt petrogenesis: a study of quartz tholeiites to olivine melilitites from southeastern Australia utilizing geochemical and experimental petrologic data. *J PETROL* **19**, 463–513.
- Gill, J. B. 1981. *Orogenic andesites and plate tectonics*. New York: Springer-Verlag.
- Green, T. H. 1982. Anatexis of mafic crust and high pressure crystallization of andesite. In Thorpe, R. S. (ed.) *Andesites—orogenic andesites and related rocks*, 465–87. New York: Wiley.
- Green, T. H. & Ringwood, A. E. 1968. Genesis of the calc-alkaline igneous rock suite. *CONTRIB MINERAL PETROL* **18**, 105–62.
- Hacker, B. R. 1990. Amphibolite-facies-to-granulite-facies reactions in experimentally deformed, unpowdered amphibolite. *AM MINERAL* **75**, 1349–61.
- Harmon, R. S., Barreiro, B. A., Moorbath, S., Hoefs, J., Francis, P. W., Thorpe, R. S., Deruelle, B., McHugh, J. & Viglino, J. A. 1984. Regional O-, Sr-, and Pb-isotope relationships in late Cenozoic calc-alkaline lavas of the Andean Cordillera. *J GEOL SOC LONDON* **141**, 803–22.
- Helz, R. T. 1976. Phase relations of basalts in their melting ranges at $P_{H_2O} = 5$ kb. Part II. Melt composition. *J PETROL* **17**, 139–93.
- Hochstaedter, A. G., Kepezhinskas, P. K., Defant, M. J., Drummond, M. S. & Bellon, H. 1994. On the tectonic significance of arc volcanism in northern Kamchatka. *J GEOL* **102**, 639–54.
- Hole, M. J., Saunders, A. D., Murriner, G. F. & Tarney, J. 1984. Subduction of pelagic sediments: implications for the origin of Ce-anomalous basalts from the Mariana Islands. *J GEOL SOC LONDON* **141**, 453–72.
- Holland, T. J. B. 1979. Experimental determination of the reaction paragonite = jadeite + kyanite + H₂O, and internally consistent thermodynamic data for part of the system Na₂O–Al₂O₃–SiO₂–H₂O, with applications to eclogites and blueschists. *CONTRIB MINERAL PETROL* **68**, 293–301.
- Holloway, J. R. & Burnham, C. W. 1972. Melting relations of basalt with equilibrium water pressure less than total pressure. *J PETROL* **13**, 1–29.
- Ishizaka, K. & Carlson, R. W. 1983. Nd–Sr systematics of the Setouchi volcanic belt, southwest Japan: a clue to the origin of orogenic andesite. *EARTH PLANET SCI LETT* **64**, 327–40.
- Jahn, B. M., Gliksun, A. Y., Peucat, J. J. & Hickman, A. H. 1981. REE geochemistry and isotopic data of Archean silicic volcanics and granitoids from the Pilbara Block, Western Australia: implications for the early crustal evolution. *GEOCHIM COSMOCHIM ACTA* **45**, 1633–52.
- Jahn, B. M., Vidal, P. & Kroner, A. 1984. Multi-chronometric ages and origin of Archean tonalitic gneisses in Finnish Lapland: a case for long crustal residence time. *CONTRIB MINERAL PETROL* **86**, 398–408.
- Johnston, A. D. & Wyllie, P. J. 1989. The system tonalite–peridotite–H₂O at 30 kbar with applications to hybridization in subduction zone magmatism. *CONTRIB MINERAL PETROL* **102**, 257–64.
- Kay, R. W. 1978. Aleutian magnesian andesites: melts from subducted Pacific ocean crust. *J VOLCANOL GEOTHERM RES* **4**, 117–32.

- Kay, R. W. & Kay, S. M. 1991. Creation and destruction of lower continental crust. *GEOL RUNDSCH* **80**, 259–78.
- Kay, R. W. & Kay, S. M. 1993. Delamination and delamination magmatism. *TECTONOPHYSICS* **219**, 177–89.
- Kay, S. M., Mpodozis, C., Ramos, V. A. & Munizaga, F. 1991. Magma source variations for mid–late Tertiary magmatic rocks associated with a shallowing subduction zone and a thickening crust in the central Andes (28° to 33°S). *GEOL SOC AM SPEC PAP* **265**, 113–38.
- Kay, S. M., Ramos, V. A. & Marquez, M. 1993. Evidence in Cerro Pampa volcanic rocks for slab melting prior to ridge–trench collision in southern South America. *J GEOL* **101**, 703–14.
- Kelemen, P. B. 1995. Genesis of high Mg# andesites and the continental crust. *CONTRIB MINERAL PETROL* **120**, 1–19.
- Kepezhinskas, P. K. 1989. Origin of the hornblende andesites of northern Kamchatka. *INT GEOL REV* **26**, 246–52.
- Kepezhinskas, P. K., Defant, M. J. & Drummond, M. S. 1995. Na metasomatism in the island arc mantle by slab melt–peridotite interaction: evidence from mantle xenoliths in the north Kamchatka arc. *J PETROL* **36**, 1505–27.
- Kepezhinskas, P. K., Defant, M. J. & Drummond, M. S. 1996. Progressive enrichment of island arc mantle by melt–peridotite interaction inferred from Kamchatka xenoliths. *GEOCHIM COSMOCHIM ACTA* **60**, 1217–29.
- Kepezhinskas, P. K., McDermott, F., Defant, M. J., Hochstaedter, A., Drummond, M. S., Hawkesworth, C., Koloskov, A., Maury, R. C. & Bellon, H. Trace element and Sr–Nd–Pb isotope geochemistry of the Kamchatka volcanic arc, Russia. *GEOCHIM COSMOCHIM ACTA*, in press.
- Kushiro, I. 1990. Partial melting of mantle wedge and evolution of island arc crust. *J GEOPHYS RES* **95**, 15929–39.
- Luais, B. & Hawkesworth, C. J. 1994. The generation of continental crust: an integrated study of crust-forming processes in the Archaean of Zimbabwe. *J PETROL* **35**, 43–93.
- Marsh, B. D. & Carmichael, I. S. E. 1974. Benioff zone magmatism. *J GEOPHYS RES* **79**, 1196–206.
- Martin, H. 1986. Effect of steeper Archean geothermal gradient on geochemistry of subduction-zone magmas. *GEOLOGY* **14**, 753–56.
- Martin, H. 1987. Petrogenesis of Archean trondhjemites, tonalites, and granodiorites from eastern Finland: major and trace element geochemistry. *J PETROL* **28**, 921–53.
- Martin, H. 1993. The mechanisms of petrogenesis of the Archean continental crust—comparison with modern processes. *LITHOS* **30**, 373–88.
- Massone, H. J. & Schreyer, W. 1987. Phengite geobarometry based on the limiting assemblage with K-feldspar, phlogopite, and quartz. *CONTRIB MINERAL PETROL* **96**, 212–24.
- McLennan, S. M. & Taylor, S. R. 1982. Geochemical constraints on the growth of the continental crust. *J GEOL* **90**, 347–61.
- Meijer, A. 1983. The origin of low-K rhyolites from the Mariana frontal arc. *CONTRIB MINERAL PETROL* **83**, 45–51.
- Morris, P. A. 1995. Slab melting as an explanation of Quaternary volcanism and aseismicity in southwest Japan. *GEOLOGY* **23**, 395–8.
- Mysen, B. O. 1982. The role of mantle anatexis. In Thorpe, R. S. (ed.) *Andesites–orogenic andesites and related rocks*, 489–522. New York: Wiley.
- Nelson, E. P. & Forsythe, R. D. 1989. Ridge collision at convergent margins: implications for Archean and post-Archean crustal growth. *TECTONOPHYSICS* **161**, 307–15.
- Nisbet, E. G. 1987. *The young earth*. Boston: Allen and Unwin.
- Obata, M. & Thompson, A. B. 1981. Amphibole and chlorite in mafic and ultramafic rocks in the lower crust and upper mantle. *CONTRIB MINERAL PETROL* **77**, 74–81.
- Parsons, B. A. & Sclater, J. G. 1977. An analysis of the variation of ocean floor bathymetry and heat flow with ages. *J GEOPHYS RES* **82**, 803–27.
- Peacock, S. M. 1990a. Fluid processes in subduction zones. *SCIENCE* **248**, 329–37.
- Peacock, S. M. 1990b. Numerical simulation of metamorphic pressure–temperature–time paths and fluid production in subducting slabs. *TECTONICS* **9**, 1197–211.
- Peacock, S. M., Rushmer, T. & Thompson, A. B. 1994. Partial melting of subducting oceanic crust. *EARTH PLANET SCI LETT* **121**, 227–44.
- Pearce, J. A. & Peate, D. W. 1995. Tectonic implications of the composition of volcanic arc magmas. In Wetherill, G. W., Albee, A. L. & Burke, K. C. (eds) *ANNU REV EARTH PLANET SCI* **25**, 1–85.
- Pearce, J. A., van der Laan, S. R., Arculus, R. J., Murton, B. J. & Ishii, T. 1992. Boninite and harzburgite from ODP Leg 125 (Bonin–Mariana forearc): a case study of magma genesis during the initial stages of subduction. In Fryer, P., Pearce, J. A. & Stokking, L. B. (eds) *Proceedings ODP Scientific Results, Leg 125*, 623–59.
- Philippot, P. 1993. Fluid–melt–rock interaction in mafic eclogites and coesite-bearing metasediments: constraints on volatile recycling during subduction. *CHEM GEOL* **108**, 93–112.
- Philippot, P. & Selverstone, J. 1991. Trace-element-rich brines in eclogitic veins: implications for fluid composition and transport during subduction. *CONTRIB MINERAL PETROL* **106**, 417–30.
- Poli, S. 1993. The amphibolite–eclogite transformation: an experimental study on basalt. *AM J SCI* **293**, 1061–107.
- Puga, E., Diaz de Federico, A. & Demant, A. 1995. The eclogitized pillows of the Betic Ophiolitic Association: relics of the Tethys Ocean floor incorporated in the Alpine chain after subduction. *TERRA REV* **7**, 31–43.
- Raheim, A. & Green, D. H. 1975. P,T paths of natural eclogites during metamorphism—a record of subduction. *LITHOS* **8**, 317–28.
- Rapp, R. P. 1990. *Vapor-absent partial melting of amphibolite/eclogite at 8–32 kbar: implications for the origin and growth of the continental crust*. Troy. Unpublished Ph.D. Thesis, Rensselaer Polytechnic Institute.
- Rapp, R. P. 1995. Amphibole-out phase boundary in partially melted metabasalt, its control over liquid fraction and composition, and source permeability. *J GEOPHYS RES* **100**, 15601–18.
- Rapp, R. P. & Watson, E. B. 1995. Dehydration melting of metabasalt at 8–32 kbar. Implications for continental growth and crust–mantle recycling. *J PETROL* **36**, 891–931.
- Rapp, R. P., Watson, E. B. & Miller, C. F. 1991. Partial melting of amphibolite/eclogite and the origin of Archean trondhjemites and tonalites. *PRECAMBRIAN RES* **51**, 1–25.
- Reymer, A. & Schubert, G. 1984. Phanerozoic addition rates to the continental crust and crustal growth. *TECTONICS* **3**, 63–77.
- Ringwood, A. E. 1975. *Composition and petrology of the earth's mantle*. New York: McGraw-Hill.
- Rushmer, T. 1991. Partial melting of two amphibolites: contrasting experimental results under fluid-absent conditions. *CONTRIB MINERAL PETROL* **107**, 41–59.
- Rushmer, T., Pearce, J. A., Ottolini, L. & Bottazzi, P. 1994. Trace element behavior during slab melting: experimental evidence. *EOS, TRANS AM GEOPHYS UNION* **75**, 746.
- Sajona, F. Z., Maury, R. C., Bellon, H., Cotten, J., Defant, M. J. & Pubellier, M. 1993. Initiation of subduction and the generation of slab melts in western and eastern Mindanao, Philippines. *GEOLOGY* **21**, 1007–10.
- Saunders, A. D., Rogers, G., Marriner, G. F., Terrell, D. J. & Verma, S. P. 1987. Geochemistry of Cenozoic volcanic rocks, Baja California, Mexico: implications for the petrogenesis of post-subduction magmas. *J VOLCANOL GEOTHERM RES* **32**, 223–45.
- Schreyer, W. 1988. Experimental studies on metamorphism of crustal rocks under mantle pressures. *MINERAL MAG* **52**, 1–26.
- Selverstone, J., Franz, G., Thomas, S. & Getty, S. 1992. Fluid variability in 2 GPa eclogites as an indicator of fluid behavior during subduction. *CONTRIB MINERAL PETROL* **112**, 341–57.
- Sen, C. & Dunn, T. 1994. Dehydration melting of a basaltic composition amphibolite at 1.5 and 2.0 GPa: implications for the origin of adakites. *CONTRIB MINERAL PETROL* **117**, 394–409.
- Sen, C. & Dunn, T. 1995. Experimental modal metasomatism of a spinel lherzolite and the production of amphibole-bearing peridotite. *CONTRIB MINERAL PETROL* **119**, 422–32.
- Sørensen, S. S. 1988. Petrology of amphibolite-facies mafic and ultramafic rocks from the Catalina Schist, southern California: metasomatism and migmatization in a subduction zone metamorphic setting. *J METAMORPHIC GEOL* **6**, 405–35.
- Sørensen, S. S. & Grossman, J. N. 1989. Enrichment of trace elements in garnet amphibolites from a paleo-subduction zone: Catalina Schist, southern California. *GEOCHIM COSMOCHIM ACTA* **53**, 3155–77.
- Spulber, S. D. & Rutherford, M. J. 1983. The origin of rhyolite and plagiogranite in oceanic crust: an experimental study. *J PETROL* **24**, 1–25.
- Stern, C. R., Futa, K. & Muehlenbachs, K. 1984. Isotope and trace element data for orogenic andesites from the Austral Andes. In Harmon, R. S. & Barriero, B. A. (eds) *Andean magmatism—chemical and isotopic constraints*. 31–46. Cheshire: Shiva.

- Tatsumi, Y. & Eggins, S. 1995. *Subduction zone magmatism*. Oxford: Blackwell.
- Tatsumi, Y. & Ishizaka, K. 1982. Origin of high-magnesian andesites in the Setouchi volcanic belt, southwest Japan, I. Petrographic and chemical characteristics. *EARTH PLANET SCI LETT* **60**, 293–304.
- Tatsumi, Y. & Nakamura, N. 1986. Composition of aqueous fluid from serpentine in the subducted lithosphere. *GEOL J* **20**, 191–96.
- Tatsumi, Y., Hamilton, D. L. & Nesbitt, R. W. 1986. Chemical characteristics of fluid phase released from a subducted lithosphere and origin of arc magmas: evidence from high-pressure experiments and natural rocks. *J VOLCANOL GEOTHERM RES* **29**, 293–309.
- Taylor, S. R. & McLennan, S. M. 1985. *The continental crust: its composition and evolution*. Oxford: Blackwell.
- Taylor, R. N., Nesbitt, R. W., Vidal, P., Harmon, R. S., Auvray, B. & Croudace, I. W. 1994. Mineralogy, chemistry, and genesis of the boninite series volcanics, Chichijima, Bonin Islands, Japan. *J PETROL* **35**, 577–617.
- Thompson, A. B. & Ellis, D. J. 1994. CaO + MgO + Al₂O₃ + SiO₂ + H₂O to 35 kb: amphibole, talc, and zoisite dehydration and melting reactions in the silica-excess part of the system and their possible significance in subduction zones, amphibolite melting, and magma fractionation. *AM J SCI* **294**, 1229–89.
- Tsuchiya, N. & Kanisawa, S. 1994. Early Cretaceous Sr-rich silicic magmatism by slab melting in the Kitakami Mountains, northeast Japan. *J GEOPHYS RES* **99**, 22 205–20.
- Ulmer, P. & Trommsdorff, V. 1995. Serpentine stability to mantle depths and subduction-related magmatism. *SCIENCE* **268**, 858–61.
- Wedepohl, K. H. 1995. The composition of the continental crust. *GEOCHIM COSMOCHIM ACTA* **59**, 1217–32.
- Winther, K. T. & Newton, R. C. 1991. Experimental melting of hydrous low-K tholeiite: evidence on the origin of Archean cratons. *BULL GEOL SOC DENMARK* **39**, 213–28.
- Wolf, M. B. & Wyllie, P. J. 1991. Dehydration-melting of solid amphibolite at 10 kbar: textural development, liquid interconnectivity and applications to the segregation of magmas. *MINERAL PETROL* **44**, 151–79.
- Wolf, M. B. & Wyllie, P. J. 1994. Dehydration-melting of amphibolite at 10 kbar: the effects of temperature and time. *CONTRIB MINERAL PETROL* **115**, 369–83.
- Wyllie, P. J. 1982. Subduction products according to experimental prediction. *GEOL SOC AM BULL* **93**, 468–76.
- Wyllie, P. J. 1984. Sources of granitoid magmas at convergent plate boundaries. *PHYSICS EARTH PLANET INTER* **35**, 12–8.
- Yogodzinski, G. M., Volynets, O. N., Koloskov, A. V., Seliverstov, N. I. & Matuenkov, V. V. 1994. Magnesian andesites and the subduction component in a strongly calc-alkaline series at Piip volcano, far western Aleutians. *J PETROL* **35**, 163–204.
- Yogodzinski, G. M., Kay, R. W., Volynets, O. N., Koloskov, A. V. & Kay, S. M. 1995. Magnesian andesite in the western Aleutian Komandorsky region: implications for slab melting and processes in the mantle wedge. *GEOL SOC AM BULL* **107**, 505–19.

MARK S. DRUMMOND, Department of Geology, University of Alabama at Birmingham, Birmingham, AL 35294-2160, U.S.A.

MARC J. DEFANT, Department of Geology, University of South Florida, Tampa, FL 33620-5200, U.S.A.

PAVEL K. KEPEZHINSKAS, Department of Geology, University of South Florida, Tampa, FL 33620-5200, U.S.A.